GAS PRESSURE IN ALUMINUM BLOCK WATER JACKET CORES

A. Starobin
Flow Science, Inc., Santa Fe, NM, USA
Currently under a Research Contract with the American Foundry Society

D. Goettsch
GM Powertrain, Pontiac, MI, USA

M. Walker
GM R&D Center, Warren, MI, USA

D. Burch
Alchemcast LLC, Birmingham, AL, USA

Abstract

Thermophysical properties of mixture gas are computed from prior laboratory pyrolysis studies of polyurethane cold-box binder (PUCB) performed by Lytle, Bertsch and McKinley.[1] This gas is found to have an overall gas constant of 230 J/kg/C. Controlled aluminum submersion tests of a PUCB bonded water jacket core yield values of gas pressure at discrete points during fill of an engine-block casting. These are found in adequate agreement with predictions of a physical model that considers details of binder pyrolysis and product gas transport in the sand core.

Keywords: thermal degradation of binders, core gas pressure prediction, aluminum casting gas defects

Introduction

In general in foundry practice it is difficult to identify the source of the gas defects in the finished casting. Possible sources of gas include atmospheric gases entrained during pour, gases dissolved in the metal, water vapor from green sand molds blown back into the casting, gases evolved from core and mold coatings and gases produced in the course of core binder pyrolysis. The physical and numerical modeling of the casting process offers an opportunity to study each source of gas independently and develop solutions to reduce the occurrence of gas defects.

This work examines the role of core binder gas in defect formation in aluminum castings and shows significant progress from previous attempts to quantitatively understand core gas pressure.[2,4] Specific focus is on the gases generated through pyrolysis of polyurethane cold-box Isocure® binder (hereafter simply referred to as a PUCB binder) under aluminum casting conditions. The physical description and the computational approach taken are general and could be used for other binders and other metal castings if the necessary data is available.

The specific goals were to take the detailed laboratory data on the pyrolysis of the binder, [1,3] deduce the essential physical input, and use this input along with the detailed knowledge of core geometry and the filling sequence to make predictions of core gas pressure. The computed pressure values are compared against pressures obtained from the combination of foundry core submersion tests and real-time X-ray recordings of gas blow performed at the General Motors Corporation.

Parameters Affecting Core Gas Pressure

The basic estimate for peak core gas pressure goes back to Campbell's description of binder gas generation and transport.[6] Essentially a thin pyrolysis zone develops near the surface of the core as the metal fills the casting cavity. The products of pyrolysis are then transported from the core surface to the core prints down the gas pressure gradient. Along the flow path large temperature variations are expected as the pyrolysis range of a typical resin binder is well above room temperature.

As a general rule, the peak gas pressure is proportional to the pyrolysable binder density in the core, ρ_b. It is also proportional to the total core area exposed to the metal, A_c, and to the mean speed of the pyrolysis zone into the core, u_p. This speed is a complex quantity that depends on the binder, on the metal cast and on the shape and immersion history of the core.

With a fixed pyrolysis rate, a lighter gas, or equivalently gas with a larger gas constant, R_g, gives rise to a larger volume and larger flow velocities. The chocking cross-section of the core, ϕA_p, typically at core prints, determines peak flow velocity which can then be related to peak core gas pressure. Only a fraction of the geometric area is open to gas flow, hence A_p is scaled by the core porosity ϕ.

Further, higher pressure losses are expected for gas mixtures of higher viscosity, μ_g, and for cores with smaller intrinsic permeability, K, such as obtained in finer grade/larger AFS number sand cores. Finally, the peak gas pressure will increase as the maximum distance from core surface to the print, L, is increased.

The described relationships can be summarized in an approximate equation for peak gas pressure in a given core:

$$P \sim \left(\frac{R_g T}{P_0}\right)\left(\rho_b u_p A_c\right)\left(\frac{L \mu_g}{A_p \phi K}\right) \qquad \text{Equation 1}$$

The first bracket gives the inverse density of the transported gas. The second gives the binder loss rate and the third the pressure drop per unit volumetric flow rate. The essential difference between Equation (1) and its variant appearing in Reference 6 is the explicit form of the binder mass loss rate (2nd bracket). A pyrolysis model for PUCB binder derived from the thermo-gravimetric analysis by McKinley et al.[3] will be used to compute the pyrolysis speed for a specific core in a specific casting. Further difference is the emphasis on the role of the mixture gas constant for pressure predictions. This constant will be computed in section two from the composition analysis of the outgassing species reported in Reference 1.

The actual gas pressure developing in a core will be limited by the combined confining metal flow pressure at the core wall, P_m, and a typically smaller surface tension pressure:

$$P_g \leq P_m + \frac{2\gamma}{R} \qquad \text{Equation 2}$$

where γ is the surface tension of the metal, including possible effects of the oxide film and solidified skin, and R is the size of the gas bubble generated when core gas is blown into the casting. In general one cannot deduce gas pressures from the right hand side of Equation (2), for it only provides an upper bound. In the special case of a mechanical balance, or right after the gas is sealed in the core, the gas pressure is known.

Physical Description of the PUCB Binder Gas

The essential properties of the binder gas for core pressure prediction are the mixture gas constant (R_g) and the mixture gas viscosity (μ_g). These can be calculated from detailed composition data obtained in laboratory isothermal pyrolysis studies of Lytle et al.[1] The light volatile compounds and their relative quantities produced in a 900C (1652F) pyrolysis experiment are listed in Table 1. These were found to account for 99.9% of all volatiles detected at the temperature of the experiment. Further, 80.8% of these by weight and 92.3% by molar content remain volatile down to room temperature. Of the three compounds that are semi-volatile -(1-pentene, 1,3-pentadiene and 2-propenenitrile)—the highest normal boiling point is 77C (171F), which suggests that these compounds, at least partially will be volatilized during transport through the heated cores. The molar fractions, χ_i, and molar masses, M_i, of species in Table 1 can be combined according to Equation (3) to obtain the mean molar mass of the gas, $\overline{M}$, and its gas constant;

$$\overline{M} = \sum_i \chi_i M_i, \quad R_g = \frac{R_0}{\overline{M}} \qquad \text{Equation 3}$$

to give ranges 36.1-38.6 g/mol, and 215-230 J/kg/K for molar mass and the gas constant respectively. The higher value of the gas constant corresponds to the species still volatile at room temperature.

In aluminum castings the highest-achieved sand core temperature will be lower than 900C (1652F). Additional composition data is available from a parallel study by McKinley[3] on the PUCB binder at a lower pyrolysis temperature of 700C (1292F). The main volatile products are the same, though relative amounts differ. Most importantly for this study, the gas constant remains essentially the same, now 228 J/kg/C for gases volatile at room temperature (about 91 % by mole faction).

The mole-fraction-weighted estimate of gas viscosity at room temperature from Table 1 is 1.1×10^{-5} Pa s, considerably lower than the viscosity of air. At an elevated temperature of 230C (446F), consistent with mean temperature conditions in casting sand cores, the viscosity is estimated to be as high as 1.6×10^{-5} Pa s.

Pyrolysis Rate of Resin Binder in Aluminum Castings

The measurements of Lytle et al.[1] and McKinley[3] also provide data needed for computation of the rate of binder pyrolysis. Specifically, these authors performed thermo-gravimetric analysis (TGA) at a fixed heating rate of 150C/min (302F/min). The mass loss rate curve peaked roughly at 230C (446F) and no more mass change was observed above 680C (1256F). The residue fraction was 30%. The actual rate of mass loss curve had multiple peaks. McKinley[3] identifies nine, each one parametrized by the weight fraction attributed to the peak, $\Delta\omega_i$, and by two first-order Arrhenius reaction parameters, E_i and C_i. This parameterization is reproduced in Table 2.

The total pyrolysis rate of the binder, $\dot{\rho}$, is then given as the sum over the actions of the individual rates, $\dot{o}_i$:

$$\dot{o}_i = -\dot{o}_i\, C_i \exp\left\{-\frac{E_i}{R_0 T}\right\},\ \dot{\rho} = \rho_b \sum_i \Delta\omega_i \dot{o}_i \quad \text{Equation 4}$$

where ρ_b is the initial binder density in the core which can also be written as a product of the initial binder fraction and the density of the sand.

The first rate identified in[3] can be shown to be active already at room temperature. Specifically the exponential decay time for $\Delta\omega_1$ is 570 seconds in a room temperature holding experiment. This indicates a fast outgassing reaction such as possibly volatilization of the solvent right after the core is hardened.

The rest of the rates in Table 2 will only produce an appreciable amount of gas products under casting conditions. The temperature range in which each rate would be active in a 20C/s (68F/s) steady heating experiment is given in columns four and five of Table 2. A multi-rate model is generally required to accurately represent the wide temperature range of this pyrolysis process.

To further highlight the features of the model, the pyrolysis speed and binder fraction are computed for a simple flat wall case. In this numerical experiment, aluminum at 720C (1328F) is at the sand core wall at t=0. The heat transfer coefficient to sand is 500 W/m^2 /C, in the range of previously reported values.[8] Because the binder fraction is low, the heat capacity of the bonded core sand should be well approximated by values for dry silica sand.[9] The thermal conductivity was measured directly in the course of this work with the aid of a transient plane source thermal conductivity system TPS 2500 S.[10] It was found to track thermal conductivity values of the green molding sand to 300C (572F). The PUCB bonded core sand had lower thermal conductivity above 300C (572F), with the largest difference of 30% at 500C (932F).[9,10]

The results of the numerical pyrolysis experiment are plotted in Figure 1. On the right is the binder fraction in the wall at 7, 15 and 30 seconds. It can be seen that the residue fraction is 40% and the middle of the pyrolysis zone moves into the core wall at approximately 0.1 mm/s. The computed pyrolysis speed is plotted on the left of Figure1 and shows a peak of 0.13 mm/s at 1.6 seconds and a decay to a value of 0.075 mm/s at 30 seconds. As the pyrolysis zone moves away from

Table 1. Volatile Chemical Compounds Identified by Lytle et al.[1] in a GC/MS Analysis of Pyrolysis of PUCB Isocure® Performed at 900C (1652F). 92.3% (by Molar Content) of These are Still Volatile at Room Temperature and the Gas Constant for this Mixture is 230 J/kg/C

Volatile Compounds	Chemical Formula	Weight fractions	Molar mass (g/mol) M_i	Molar fractions χ_i	Standard Boiling Point (C)*	RT Component visc. (x10^{-5} Pa s)*	230 C Component visc. (x10^{-5} Pa s)*
Carbon Monoxide	CO	0.143	28	0.197	-161	1.75	2.5
Propene (Propelyne)	C_3H_6	0.304	42	0.279	-48	0.87	1.4
1-butene (Butelyne (alpha))	C_4H_8	0.115	56	0.0792	-63	0.75	1.15
1-pentene (Amylene)	C_5H_{10}	0.071	70	0.039	30	0.7	1.1
Methane	CH_4	0.0533	16	0.1285	-191	1.12	1.7
1,3-butadiene:	C_4H_6	0.092	54	0.0657	-4.4	0.55**	1**
1,3-pentadiene(piperylene)	C_5H_8	0.096	68	0.0547	42	0.55**	1**
Ethene (Ethylene)	C_2H_4	.101	28	0.139	-104	1	1.6
2-propenenitrile	CH2CHCN	0.024	53	0.0174	77	0.55**	1**
Volatile balance		0.1	~100	0.0005		0.55**	1**

*See Reference 7. **These are assumed values, for no tabulated values for these gases could be found.*

the mold-metal interface the heat input into the wall drops which accounts for the overall drop in pyrolysis speed and pyrolysis rate.

Transport of Core Gas

The gases generated through pyrolysis are transported through the core with an associated pressure loss. For the range of flow speeds expected during gas transport, Darcy's law is adequate to predict gas velocities:

$$\vec{u}_g = -\frac{K}{\mu_g(T)}\nabla p_g \qquad \text{Equation 5}$$

Here $\vec{u}_g$ is the gas flow velocity and P_g is the core gas pressure. K is the intrinsic sand permeability found to be of order $10^{-10}\ m^2$ in room temperature air flow experiments[14] (with the actual value varying inversely with the square of the sand grain size)[12] μ_g is core gas viscosity which should increase with temperature as $\propto \sqrt{T}$,[11] and P_g is the core gas pressure.

The density of the core gas simultaneously satisfies the mass transport equation and the ideal gas equation of state:

$$\frac{\partial \rho_g}{\partial t} + \nabla \bullet \left(\rho_g \vec{u}_g \right) = -\frac{d\rho}{dt} \qquad \text{Equation 6}$$

$$p_g = R_g \rho_g T \qquad \text{Equation 7}$$

where P_g and P are microscopic core gas and macroscopic core binder densities and T is the gas temperature. The specific form of the right hand side in Equation (6) is given by Equation (4). The gas density is expected to increase significantly as the gas is transported from the hot pyrolysis zone to the colder venting (e.g. print) surfaces of the core. Further, a smaller change (drop) in gas density is expected as the gas moves in the direction of lower pressure.

The thermal contact between the gas and the sand is expected to be very good given the large surface per unit volume of sand and the relatively small gas transport velocity expected. Thus we use a one-temperature model with the gas temperature taken at the temperature of the sand. The

energy advection and expansion work effects are also expected to be small. Further, as described in the previous sections, the molar content of the condensable species is small and both the effects of possible condensation/evaporation on gas density and on gas specific energy and temperature are ignored.

At the boundaries of the core two possibilities exist: either the gas is free to exit, or the gas is sealed in by the surrounding metal. This is decided with the aid of Equation (2). The bubble

Table 2. First Order Decomposition Reactions Active During Pyrolysis of a PUCB binder.[3] Fraction of binder volatilized by a given reaction–column 2, Arrhenius parameters for a given reaction–columns 3 and 4, and approximate temperature range over which a given reaction is active–columns 5 and 6

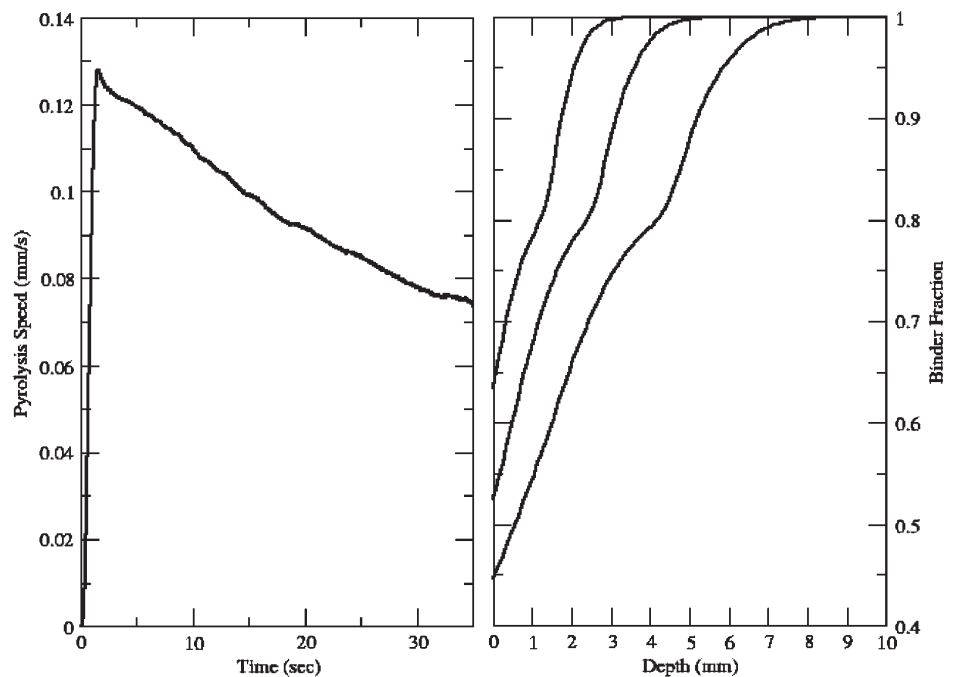|	$\Delta\omega_i$ (%)	C_i (1/sec)	E_i (kJ/mol)	T_- (C)	T_+ (C)
1	10	1.33E+005	43.9	NA	NA
2	3.6	8.33E+007	73.2	117	245
3	15.5	9.16E+007	83.7	169	312
3.1	2.8	1.67E+007	86.2	215	387
4	6.3	9.16E+006	93.3	267	463
5	9.4	2.67E+006	96.7	318	547
6	7	2.50E+006	103.3	358	603
7	11	3.00E+006	115.5	423	689
8	4.5	3.30E+006	127.6	490	777

Figure 1. Left panel: Pyrolysis speed vs. time in a PUCB bonded flat core wall immersed in Al at 720C (1328F). Right panel: The binder fraction in the mold at 7, 15 and 30 seconds. The origin is at the metal-mold interface.

dynamics is not modeled and a fixed surface tension threshold is used as an input quantity. When the equality is achieved, the boundary gas pressure is fixed and the amount of gas blown follows from Equation (5). At the core print boundaries, the pressure is fixed corresponding to perfect venting. In all cases the boundary gas density is set consistently from the boundary pressure and boundary gas temperature using Equation (7).

To model the pressure in core vents an energy balance is written for the whole vent cavity which includes advected energy and flow work done on/by the gas in the vent cavity. Unlike in the bulk of the sand, conductive heat transfer from vent gas to the surrounding core is relatively small and is neglected. Because the gas is taken as ideal the total energy of the gas in the vent (E_v) is simply related to vent pressure and vent volume (P_v, V_v):

$$E_v = \frac{3}{2} P_v V_v \qquad \text{Equation 8}$$

The rate of change of vent pressure can then be written as:

$$\dot{P}_v = -P_v \frac{5}{3} \frac{1}{V_v} \int_{\partial A_v} dA \, \bar{u}_g \, \hat{n}, \quad \text{Equation 9}$$

where the integration is performed over the vent surface ∂A_v.

Foundry Tests and Observations

A 730C, A319 alloy was pumped from below into an open flask, submerging the jacket core and allowing the observation of bubble formation. The geometry and its CAD representation are shown in Figure 2. The PUCB bonded core was a two-piece assembly of the slab, directly printed into the mold wall, and the water jacket core, printed into the slab. The jacket wall thickness ranged from 8 to 14 mm. Because of the V-engine geometry, the jacket core was at a 45 degree slant which resulted in the lower portion of the jacket submerging at 7.5 seconds and upper at 15 seconds after the beginning of flask fill. Bubbles were observed forming from lower and upper portions of the 48 cm long water jacket core as soon as the local peaks were submerged. In Figure 2 these core peaks are marked with open red circles. In a separate set of measurements the jacket was X-rayed during fill and a typical bubble size at detachment was seen to be 0.75 cm.

When sufficient metal height was built up over the core the bubbling stopped. To suppress the bubbling from the lower and upper core portions, 7.5 cm and 12.5 cm of metal head was required (measured from the respective core peaks). Though the water jacket core is geometrically symmetric,

Table 3. Thermophysical Data Used to Compute Gas Pressures

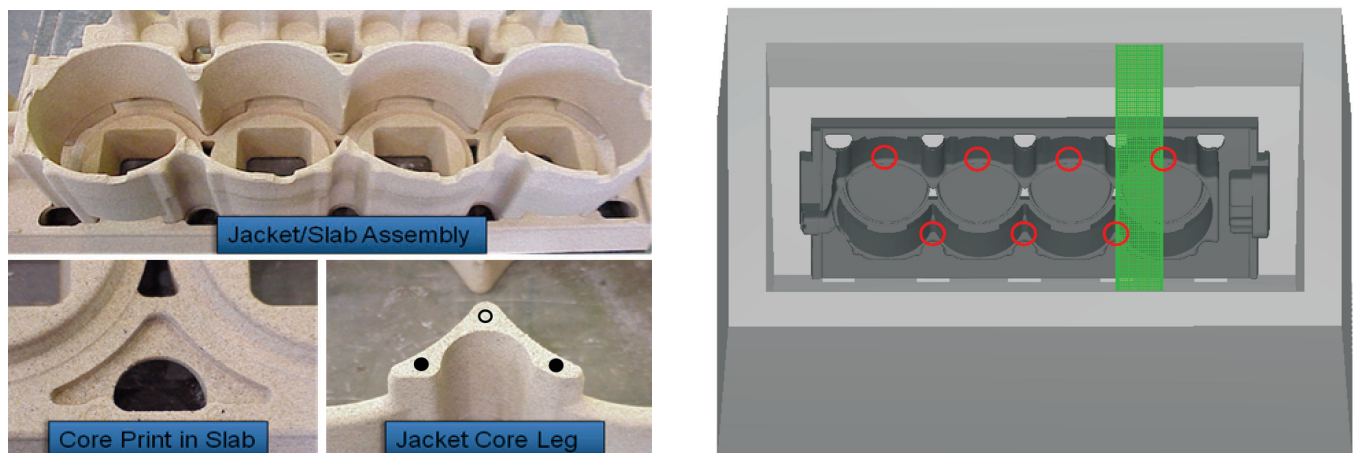| Thermophysical Data	
R_g	230 J/kg/C
μ_g at room temperature	1.1×10^{-5} Pa s
Permeability	4.17×10^{-11} m^2 (Ref.15)
Sand Density	1540 kg/m^3
Binder Content By Weight	1.3%
Binder Ougassed During Casting	60%
Core Porosity	40%
Heat Transfer Coefficient (metal-to-core)	500 W/m^2/C (Ref.9)
Thermal Conductivity of Bonded Sand	(Ref. 11)
Heat Capacity of Bonded Sand	(Ref. 10)
Metal Density	2430 kg/m^3

Figure 2. Left panel: Details of core geometry. The standard jacket core is not vented. For the vented jacket, the locations of vent drills on the core leg are marked with black circles (solid black for the two vents per leg in the upper jacket and open circle for one vent per leg in the lower jacket). Right panel: CAD model of the flask (light grey), slab/water-jacket assembly (dark grey) and the simulation domain (light green). Five metal gates into the flask are visible just below the slab core. The lower and upper core peaks where gas bubbles were seen to detach are marked with open red circles.

due to the core slant and due to the opening of the flask, it takes longer to build up a given metal head over the upper core portion. This results in an overall higher core temperature at seal and therefore a higher gas pressure. This is further illustrated in the left panel of Figure 4, where we plot simulated metal height history in the mold. While the metal flow rate into the flask is near constant, the rate of head change drops from 3.5 cm/s to 0.8 cm/s during fill.

A method was devised to eliminate gas blow into the metal by providing vents drilled into the water jacket core from the prints. The vent channels were 90 mm long and 1.5 mm in diameter. Two were provided per upper jacket leg and one per lower (see Figure 2 for vent locations). The absence of gas blow from the vented jacket implies that the gas pressure at core peaks right after submersion is at, or below the metal surface tension threshold (second term on the right hand side of Equation 2)

Numerical Computation of Core Gas Pressure

The numerical computation of core gas pressure in the water jacket-slab core assembly was carried out in the symmetry reduced portion of the geometry as indicated in Figure 2. The physical model described above was discretized on a finite-volume mesh in the core interior. The fluid flow equations were concurrently solved in the casting cavity, so that the metal filling pattern was computed simultaneously with binder pyrolysis and gas transport. The thermo-physical values used in the computations are summarized in Table 3.

A conservative first-order numerical method was used to compute temperatures in the mold and the metal, SOLA-VOF algorithm was used to solve metal momentum and advection equations,[5] while the compressible gas transport Equation (6) coupled with the Equation of state (7) and the Darcy law, Equation (5), were solved with a variant of the
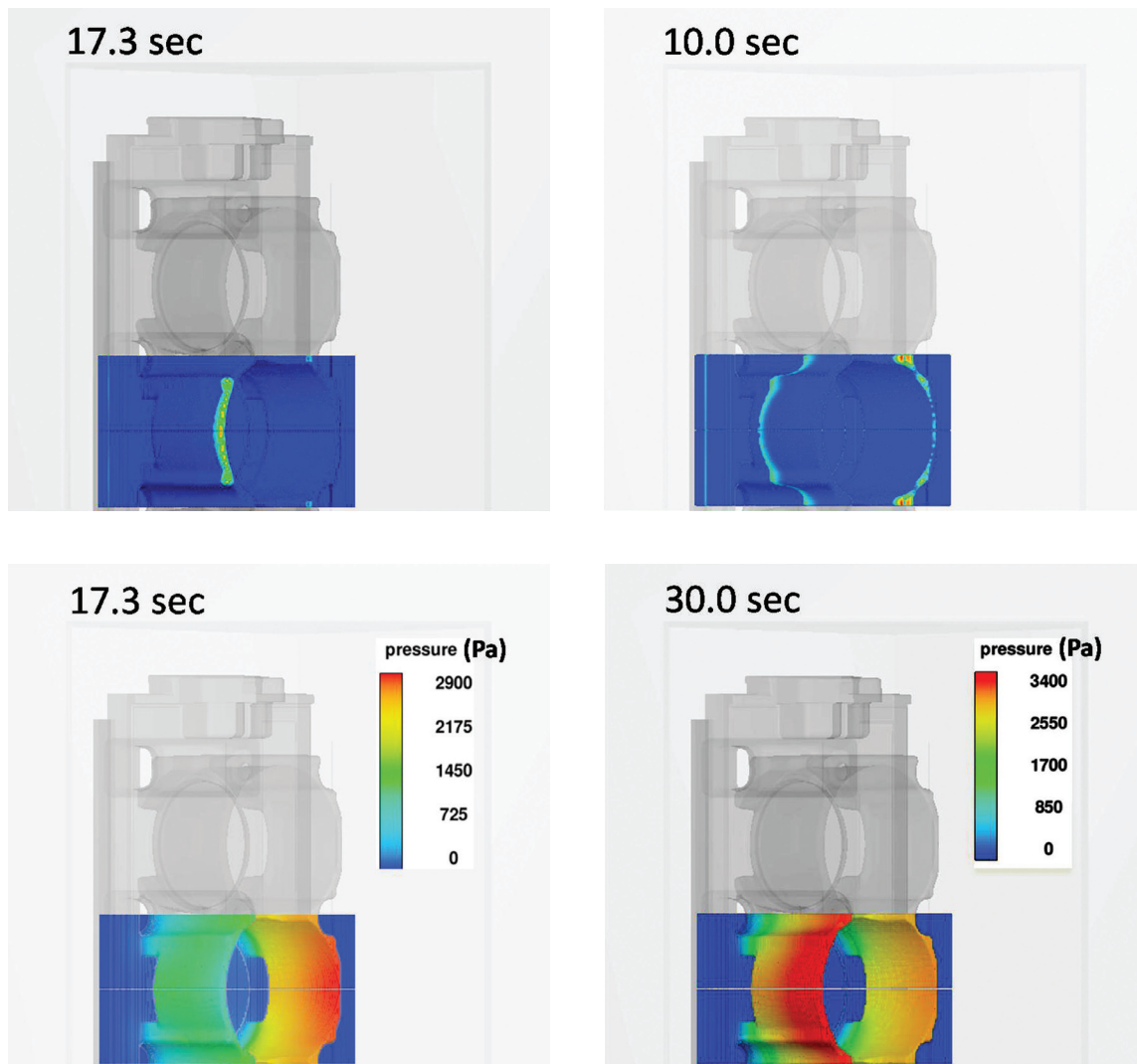

Figure 3. Bottom Row: Computed core gas gauge pressure at 17.3 and 30 seconds. Top Row: Computed locations of gas blow to metal at 17.3 and 30 s. The core submerges at 15 s and at 30 s no more gas blows to metal. The gas seals in the lower portion of the jacket at 17.5 s. As in Figure 2 red circles mark approximate locations where bubbles were blown to metal in foundry tests.

Implicit Continuous-fluid Eulerian method.[13] The asymptotic expansion of the integral of Equation (4), the pyrolysis rate equation, was found to be accurate. It was used to update binder variables every time step for every rate in Table 2.

In Table 4, a comparison is made between the two observed seal heights and the computed values. The bubbling from the core is predicted to stop with 12.1 cm of metal over the jacket in good agreement with the observed value of 12.5 cm. The needed metal head is built up at 30 seconds after the beginning of fill. At this point gas flux to metal goes to zero (Figure 4) and the gas pressure in the jacket (Figure 3) is such that at the geometric core peak the gas pressure is balanced by a combination of metal and surface tension pressures. The latter is taken to be 450 Pa, a value appropriate for the measured bubble size and a high temperature Al surface tension of 0.85 N/m.

The locations of gas blow to metal are also well captured. At 10 seconds when only the lower portion of the jacket is submerged (see Figure 4 for the timing of the submersion and seal events) the gas blows to metal along the lower rim of the core with the largest gas flux at lower core peaks. Gas also escapes ahead of the metal front in the upper portion of the jacket (Figure 3). At 15 seconds the core submerges completely and significant gas blow is correctly predicted along its upper rim.

In the simulation the gas in the lower portion of the core seals at 17.5 seconds, with 9.4 cm of metal over lower core peaks. This is higher than the observed value of 7.5 cm and this discrepancy remains unexplained.

The outgassing rate of the jacket core rises rapidly as the jacket is submerged and is very close to its peak value at submersion time. At about 22 seconds the thinner, 8 mm, sections of the core begin to pyrolyze through and the total outgassing rate begins to drop (Figure 4). The normalization adopted for the pyrolysis rate allows comparison of different cores. Per unit area and per unit binder the water jacket outgasses less than an instantaneously submerged thick flat core slab (compare Figures 1 and 4).

Table 4. Comparison of Computed and Observed Bubble-Stop Metal Heights

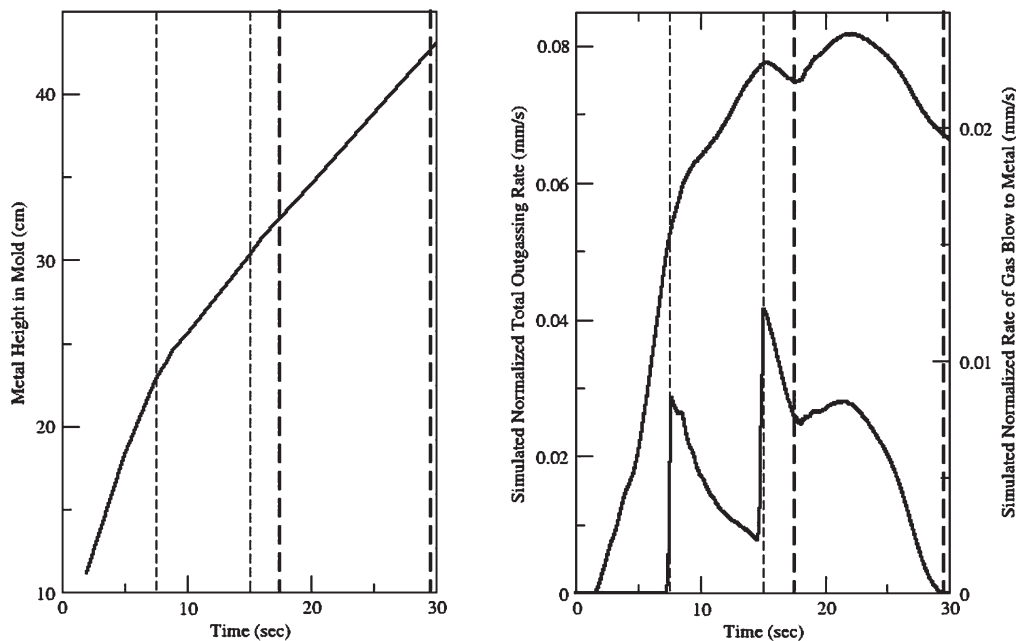| Bubble-Stop Metal Height Above:	GM Foundry Tests (cm)	Computed Values (cm)
Lower Core Peaks	7.5	9.4
Upper Core Peaks	12.5	12.1

Figure 4. Left panel: Metal height in mold during fill. Right panel: Normalized core outgassing (upper curve) and gas-to-metal blow vs. time. The mass rate is normalized by the core surface area and the bulk density of pyrolyzable binder. Fine dashed lines mark the submersion times and coarse dashed lines mark the gas seal times of the lower and upper parts of the water jacket core.

The gas blow curve in Figure 4 can be seen to track submersion and seal events. It also shows that the lower part of the jacket has a lower peak blow rate, seals faster and overall blows less gas to metal than the upper portion of the core. As a result only one vent per core leg was needed in the lower jacket to fully evacuate the gas, while two were needed for upper core legs.

Computations for the vented geometry showed no gas blow to metal when the surface tension threshold was set to 570 Pa. This is somewhat higher than the expected value of 450 Pa and could be due to the increase of the metal surface tension in the presence of an oxide skin.

Conclusions

Gas formed during pyrolysis of sand binder can be a serious source of defects in castings. Foundry core submersion tests show that gas pressure in an Al block water jacket core during casting is sufficiently low that all gas can be evacuated with proper venting. These tests further yield reference gas pressures that are used to check the accuracy of the proposed physical model for binder pyrolysis and gas transport in cores. The level of agreement between computed and measured gas pressures indicates that the model can be used to assess both the likelihood of gas blow to metal and the effectiveness of venting in complex cores.

Acknowledgements

REFERENCES

1. Lytle, C.A., Bertsch, W., McKinley, M.D., "Determination of Thermal Decomposition Products from a Phenolic Urethane Resin by Pyrolysis-Gas Chromatography-Mass Spectrometry," *Journal of High Resolution Chromatography*, vol. 21, issue 2, pp. 128-132 (1998).
2. Starobin, A., Hirt, C.W., Goettsch, D. "A Model for Binder Gas Generation and Transport in Sand Cores and Molds," *Modeling of Casting, Welding, and Solidification Processes XII*, TMS (The Minerals, Metals & Minerals Society), Warrendale, PA (2009).
3. McKinley, M.D., "Modeling of Casting Process Combustion Products," Technical Management Concepts Inc., Beavercreek, OH (1997).
4. Winardi, L., Littleton, H., Bates, C.E., "Variables Affecting Gas-Evolution Rates from Cores in Contact with Aluminum," *Foundry Management and Technology*, August (2007).
5. FLOW-3D User Manual, v9.4 (available upon request from Flow Science, Inc., Santa Fe, NM, www.flow3d.com).
6. Campbell J., *Castings*, 2nd Ed., Butterworth-Heinemann, Oxford (2003).
7. "*Perry's Chemical Engineers' Handbook*," 6th ed., pp. 3:247-250, McGraw-Hill.
8. Hwang, J.C. *et al.,* "Measurement of Heat Transfer Coefficient at Metal/Mold Interface During Casting," *AFS Transactions*, vol. 102, pp. 877-883 (1994).
9. Pehlke, R.D., Jearajan, A., Wada, H., "*Summary of Thermal Properties for Casting Alloys and Mold Materials,*" University of Michigan (1982).
10. ThermTest Inc., "Temperature Dependent Thermal Conductivity of AFS63 1.3 wt % PUCB Core Sand" (2011).
11. Hirschfelder, J.O., Curtiss, C.F., Bird, R.B., "*The Molecular Theory of Gases and Liquids,*" John Wiley & Sons (1954).
12. Bear J., "*Dynamics of Fluids in Porous Media,*" Dover Pub., N.Y. (1972).
13. Harlow, F.H. and Amsden, A.A., "A Numerical Fluid Dynamics Calculation Method for All Flow Speeds," *Journal of Computational Physics*, vol. **8**, issue 2, p. 197 (1971).
14. Winardi, L., Scarber, P., Bates, C., "Gas Flow Permeability of AFS Sands", private com. (2006).

Technical Review and Discussion

Gas Pressure in Aluminum Block Water Jacket Cores
A. Starobin, Flow Science, Inc., Santa Fe, NM
D. Goettsch, GM Powertrain Pontiac, MI, USA
M. Walker, GM R&D Center, Warren, MI, USA
D. Burch, Alchemcast LLC, Birmingham, AL, USA

Reviewers: The authors seem to make some assumptions relating to the thermal conductivity, based on Pehlke's greensand results, which would be significantly higher as a result of the water content in greensand. This issue error would benefit from greater emphasis.

Authors: We have performed direct measurements of bonded core thermal conductivity up to 600 C. The measurements were performed at and outside lab[1] with the aid of transient plane source thermal conductivity system TPS2500 S. The values, perhaps somewhat surprisingly, were found to track thermal conductivity of the green molding sand to 300 C. Above 300 C PUCB bonded core sand had lower thermal conductivity with the largest difference of 30% at 500 C. All the computations reported in this draft were performed with temperature dependent thermal conductivities and heat capacities (also see text)

[1]ThermTest Inc, 34 Melissa St., Unit #1, Fredericton, NB E3A 6W1, Canada.